Role of low-level impurities and intercalated molecular gases in the α particle radiolysis of polytetrafluoroethylene examined by static time-of-flight secondary-ion-mass spectrometery

Gregory L. Fisher[a)]
Nuclear Materials Technology (NMT-16), Los Alamos National Laboratory, P.O. Box 1663, Los Alamos, New Mexico 87545

Christopher Szakal
Department of Chemistry, The Pennsylvania State University, 104 Chemistry Building, University Park, Pennsylvania 16802

Christopher J. Wetteland
Materials Science and Technology (MST-8), Los Alamos National Laboratory, P.O. Box 1663, Los Alamos, New Mexico 87545

Nicholas Winograd
Department of Chemistry, The Pennsylvania State University, 104 Chemistry Building, University Park, Pennsylvania 16802

(Received 22 September 2005; accepted 26 December 2005; published 21 June 2006)

The structural degradation of polytetrafluoroethylene (PTFE) upon irradiation with MeV alpha (α) particles is accompanied by the proliferation of hydrogenated and oxygen-functionalized fluorocarbon species. In this article, we explore the origin of monoxide- and dioxide-functionalized fluorocarbon species that emerge upon α particle irradiation of PTFE. Samples of neat PTFE were irradiated to α doses in the range of 10^7–5×10^{10} rad using 5.5 MeV $^4He^{2+}$ ions produced in a tandem accelerator. Static time-of-flight secondary-ion-mass spectrometry (TOF-SIMS), using a 20 keV C_{60}^+ source, was employed to probe chemical changes as a function of α particle irradiation. Chemical images and high-resolution mass spectra were collected in both the positive and negative polarities. Residual gas analysis, utilized to monitor the liberation of molecular gases during α particle irradiation of the PTFE in vacuum, is discussed in relationship to the TOF-SIMS data. [DOI: 10.1116/1.2167982]

I. INTRODUCTION

In a previous article[1] we used time-of-flight secondary-ion-mass spectrometry (TOF-SIMS) to characterize the effects of α radiolysis in a polytetrafluoroethylene (PTFE) matrix. To summarize, we observed cross-linking at α doses of $<10^{10}$ rad followed by increased fragmentation and unsaturation with increasing α particle irradiation. At α doses greater than 10^{10} rad, extreme structural degradation of the polymer became evident. Based on these results, an exposure threshold of $\sim10^{10}$ rad for MeV α particles incident on PTFE was identified; nevertheless, the necessity for further investigation into the α radiolysis of PTFE was recognized. Specifically at issue are oxygen-functionalized species which were observed to appear in the mass spectra at moderate levels of α irradiation. There are several potential sources of oxygen, including ambient and intercalated gases as well as manufacturing residues, with which radiolytically produced fluorocarbon radicals may react to form oxygenated moieties.

We report here on our most recent results using TOF-SIMS to characterize monoxide- and dioxide-functionalized fluorocarbon species and elucidate their origin within the polymer matrix. We have identified intrinsic sources of oxygen in the experimental samples as being perfluorinated polyether and intercalated gases. Residual gas analysis (RGA), employed to monitor evolved gases during α particle irradiation, is discussed in association with the TOF-SIMS data. To be succinct, the RGA data and TOF-SIMS evidence of intercalated gases are not disclosed in this article but will appear in a forthcoming article.[2] In this article we focus on the identification of oxyl and peroxyl fluorocarbons and their potential formation mechanisms.

II. EXPERIMENT

Neat PTFE in 2-mm-thick sheets was purchased from Goodfellow (Berwyn, PA, USA, P/N FP303100) for use in these experiments. Specimen preparation, handling, and α particle irradiation have been fully described previously.[1] In the current study, samples were irradiated to nominal α doses of 10^7, 10^8, 10^9, 10^{10}, and 5×10^{10} rad at beam currents of 5 nA for doses $\leqslant10^8$ rad, 15 nA at a dose of 10^9 rad, and 25 nA for doses $\geqslant10^{10}$ rad. Samples used during RGA were irradiated at a beam current of 40 nA. Irradiation was performed in continuous fashion for each nominal dose with a relative error in the cumulative dose measurements of ±10%.

Evolution of H_2O, CO/N_2, O_2, and CO_2 was monitored during α particle irradiation of the samples using a

a)Author to whom correspondence should be addressed; electronic mail: glfisher@lanl.gov

quadrupole-based residual gas analyzer (Stanford Research Systems, Sunnyvale, CA, USA, P/N RGA200). The pressure versus time scans were performed under the conditions of a 1 mA emission current, a 70 V accelerating voltage, a gain of approximately 1000, and a 1 s sampling period. The ionizer of the RGA was positioned approximately 7 in. from the specimen during analysis, and the thoriated iridium filaments were thoroughly degassed prior to sample irradiation and analysis of evolved gases.

TOF-SIMS analysis was performed using a custom instrument, described in detail elsewhere,[3] approximately two weeks following irradiation. Secondary ions for mass spectral and chemical image acquisition were generated using a 20 keV C_{60}^+ ion source focused to a diameter of $\leqslant 30\ \mu$m at the sample.[4] During data acquisition the primary ion-beam conditions were a pulse width of 50 ns at 3 kHz and a dc current of 0.54 nA. The raster area was $200\times 200\ \mu m^2$ during spectrum acquisition, and $400\times 400\ \mu m^2$ during imaging. Mass spectra were acquired with the raster area completely within or outside the irradiated portion of the sample, while images were always collected at the boundary of the irradiation zone. In the course of spectrum acquisition, approximately $2.7\times 10^{11}\ C_{60}^+/cm^2$ impinged the surface of the analytical area. The total ion dose during imaging was one-fourth the total ion dose used for spectrum acquisition. In the positive polarity, analyses were performed with a nominal mass resolution ($m/\Delta m$) of ~2500 in the mass-to-charge (m/z) region below 100 m/z. The mass resolution in the negative polarity was <500 in the same mass-to-charge range. No charge compensation was used during spectrum or image acquisition.

The TOF-SIMS spectra were collected in the range of 4–1800 m/z in both the positive and negative polarities. In general, the total counts of the negative-ion spectra are <1/16 the total counts of the positive-ion spectra. A total of three samples were analyzed, each including the α radiation doses described above. Within each irradiated zone at least two different areas were analyzed. A single image was acquired at the boundary of each irradiation zone of each sample. For mass spectral features related to the polymer matrix, relative peak intensities were generally reproducible to within ±20% from sample to sample. Where quantitative correlations are made, measurements from all samples were used to determine the mean and standard deviation of the measurement. Data values greater than one standard deviation (1σ) from the estimated mean were excluded from the data set, and the mean was calculated using a minimum of three data points for each measurement. Erroneous data points are straightforwardly attributed to sample-to-sample variation and morphological roughness at α doses $\geqslant 10^{10}$ rad since sample charging was not observed to be a problem during analysis.

Peak fitting of mass spectral data was used to enable quantitative analysis of the CFO_2^+ ion (62.9882 m/z) that is discussed below. To be specific, there is an unresolved interference of $(OH)_2SiH^+$ that has a mass-to-charge ratio of 62.9904. The presence of $(OH)_2SiH^+$ in the mass spectra was presumed based on the identification of $(OH)_3Si^+$ and its homologs in the mass spectra. The resolving power, $m/\Delta m$, of the mass spectrometer would have to be in excess of 10 000 to marginally resolve the CFO_2^+ and $(OH)_2SiH^+$ isobars. Clearly, as previously noted, we cannot achieve this level of resolving power. Therefore, ORIGINPRO® 7.5 (OriginLab Corporation, Northampton, MA, USA) was used to execute a two-peak Gaussian curve fit of the unresolved peaks. All data, which are comprised of 36 spectra from six sets of analyses, were fit with residuals (R^2) of >0.99. By comparison, fitting the data with single-peak Gaussian or Lorentzian profiles, or a two-peak Lorentzian profile, resulted in residuals of <0.98. The resulting two-peak Gaussian fit data were used in the statistical analysis as described in the preceding paragraph.

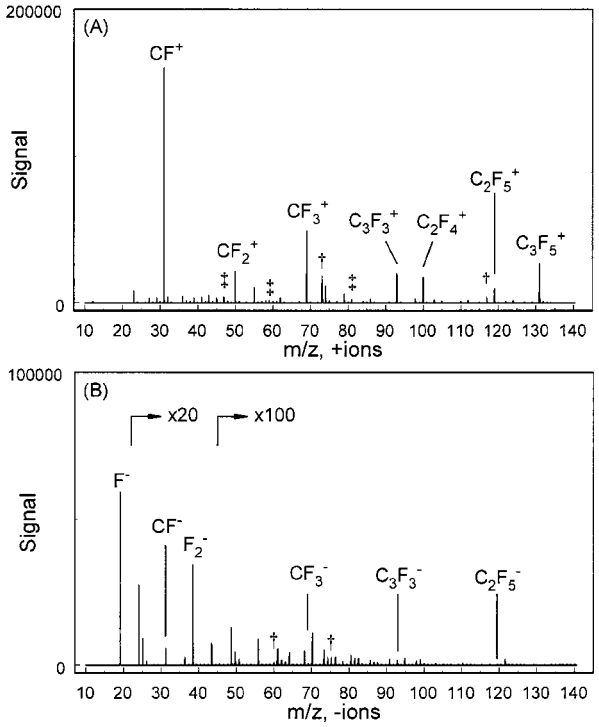

FIG. 1. TOF-SIMS spectra of unirradiated PTFE. (A) 10–140 m/z region of mass spectra acquired in the positive polarity. (B) The 10–140 m/z region of mass spectra acquired in the negative polarity. Characteristic PTFE fragment ions are indicated by formula in each spectra. Characteristic ions of silicones and perfluorinated polyethers are indicated by a cross (†) or a double cross (‡), respectively.

III. RESULTS

Analysis of the virgin PTFE specimens, shown in Fig. 1, reveals characteristic fragment ions, in both the positive and negative polarities, that are indicative of a PTFE polymer matrix with residual levels of silicones, perfluorinated polyether, common contaminants such as Na^+ (23 m/z), $^{39}K^+$ (39 m/z), $^{41}K^+$ (41 m/z), and adventitious hydrocarbons. After the initial radiation dose, the signals of characteristic PTFE fragments gradually decrease in intensity with a concurrent increase in the signal of hydrocarbon moieties. Unit mass windows at 41 and 55 m/z are shown in Fig. 2 for

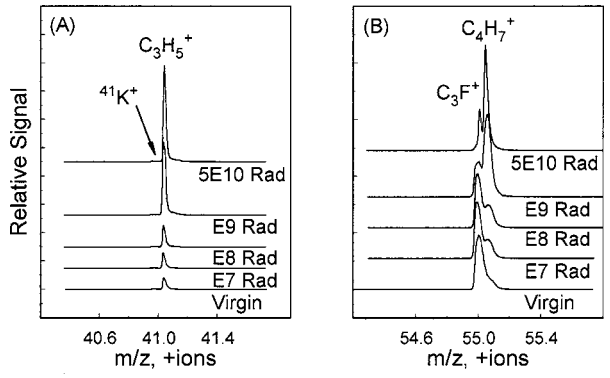

FIG. 2. Unit mass windows illustrating degradation of fluorocarbon signal and proliferation of hydrocarbons with continued α particle irradiation of the PTFE matrix. Each plot includes the raw data at experimental doses of zero, 10^7, 10^8, 10^9, and 5×10^{10} rad. (A) Positive SIMS, 41 m/z nominal. (B) Positive SIMS, 55 m/z nominal. The offset is increased at higher α doses for clarity.

comparison to the previously reported data acquired using 15 keV $^{69}Ga^+$ primary ions.[1] Each plot includes the raw signals of the unirradiated and α-irradiated samples. Potassium ($^{41}K^+$) and $C_3H_5^+$ appear at a nominal m/z of 41. The presence of $C_3H_5^+$ in the spectrum of the virgin sample is attributed to adventitious hydrocarbons. With increasing exposure of the sample to α particles, the signal of $C_3H_5^+$ increases while the signal of $^{41}K^+$ remains relatively constant. Ion-specific images of $C_3H_5^+$, displayed in Fig. 3, illustrate the connection between the rise in hydrocarbon signals and α particle irradiation. Fluorocarbon and hydrocarbon ions, C_3F^+ and $C_4H_7^+$, respectively, appear at a nominal m/z of

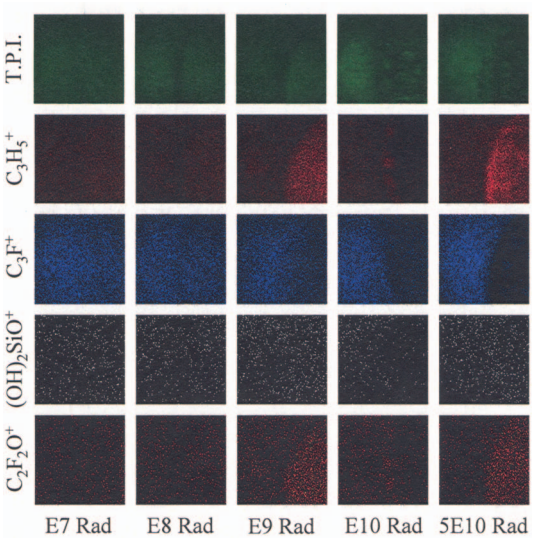

FIG. 3. Ion-specific images of α-irradiated PTFE. Image sizes are 400 $\times$400 μm^2. Within each image, the irradiated portion of the sample is to the right while the unirradiated portion is to the left. The signals of emerging species are suppressed within the 10^{10} rad irradiation zone of all samples, which is presumed to be a consequence of surface roughness. Images in each row are normalized to the same counts/pixel scale. Row 1: total positive ion (TPI) on a scale of 0–846. Row 2: $C_3H_5^+$ on a scale of 0–30. Row 3: C_3F^+ on a scale of 0–42. Row 4: $(OH)_2SiO^+$ on a scale of 0–1. Row 5: $C_2F_2O^+$ on a scale of 0–4.

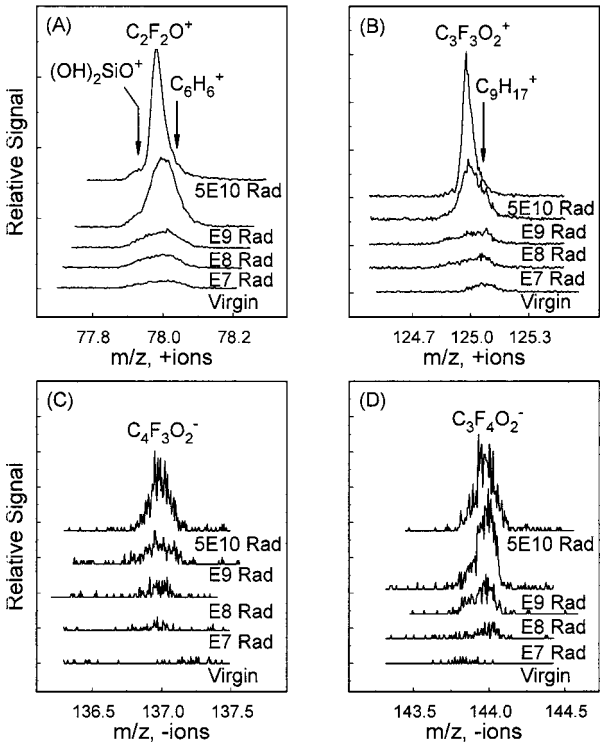

FIG. 4. Unit mass windows demonstrating the appearance and ingrowth of oxygen-functionalized fluorocarbon moieties with continued α particle irradiation of the PTFE matrix. Each plot includes the raw data at experimental doses of zero, 10^7, 10^8, 10^9, and 5×10^{10} rad. (A) Positive SIMS, 78 m/z nominal. (B) Positive SIMS, 125 m/z nominal. (C) Negative SIMS, 137 m/z nominal. (D) Negative SIMS, 144 m/z nominal. For clarity, the offset at higher α doses is increased.

55. With regard to the virgin sample, the C_3F^+ ion is characteristic of PTFE while the presence of $C_4H_7^+$ is attributed to adventitious hydrocarbons. With increasing exposure of the sample to α particles, the signal of C_3F^+ decreases while the signal of $C_4H_7^+$ increases. The decline in the C_3F^+ signal, shown in Fig. 3, is also demonstrated to be a product of α particle irradiation. These trends are in qualitative agreement with those previously reported. Thus, while improvements in signal and mass resolution have been realized using a C_{60}^+ ion probe, along with a reduction of charging artifacts, there are no discernable differences in the detected products of α particle radiolysis.

Coincident with the decline in fluorocarbon signals and proliferation of hydrocarbon signals is the observed reaction of α particle-generated fluorocarbon radicals to form oxide species. Oxygenated fluorocarbon species have been previously identified in PTFE that was irradiated with β particles.[5,6] Evidence of such species in α particle-irradiated PTFE is revealed in Fig. 4. Specifically shown are the ions $C_2F_2O^+$, $C_3F_3O_2^+$, $C_4F_3O_2^-$, and $C_3F_4O_2^-$ at nominal mass-to-charge ratios of 78, 125, 137, and 144, respectively. In the negative polarity, the oxygen-functionalized species (i.e., $C_4F_3O_2^-$ and $C_3F_4O_2^-$) emerge in the mass spectrum with the first dose of α particles and increase in intensity with increasing α dose. As demonstrated by these data, which are apparently void of isobaric interferences, only following α

particle irradiation of PTFE do the oxygen functionalities become evident. These data are supplemented by the emergence of $C_3F_3O_2^-$ (125 m/z), $C_4F_4O_2^-$ (156 m/z), and other such fragments in the negative-ion spectra upon α particle irradiation. Similarly, in the positive polarity, the signal of $C_3F_3O_2^+$ at 125 m/z appears in the mass spectrum with the first dose of α particles and increases in intensity with increasing α dose. The $C_9H_{17}^+$ isobar at 125 m/z is present at zero dose and reaches maximum intensity at 10^9 rad followed by a decrease in signal by approximately one-half at the highest α dose. The presence of $C_9H_{17}^+$ in the spectrum of the virgin sample is likely the result of isoparaffin residues in the sample matrix.[7,8]

The signal of $C_2F_2O^+$ at 78 m/z displays an increase in intensity with increasing α dose but, in contrast to the previous examples, is also present at zero dose. The appearance of $C_2F_2O^+$ at zero dose is readily explained by the existence of residual quantities of perfluorinated polyether, of which $C_2F_2O^+$ is a marker,[9] in the sample matrix. The presence of perfluorinated polyether residues is corroborated by other fragments such as CFO^+ (47 m/z), $C_2H_3O_2^+$ (59 m/z), $C_2F_3O^+$ (97 m/z), $C_2F_4O^+$ (116 m/z), and $C_2F_5O^+$ (135 m/z) that are observed in the mass spectrum. Isobaric species at 78 m/z, which include $(OH)_2SiO^+$ and $C_6H_6^+$, arising from silicone oil and isoparaffin residues, respectively, are not resolved at the lower α doses. At the highest α dose the $(OH)_2SiO^+$ isobar is marginally resolved as a shoulder on the $C_2F_2O^+$ peak, and the $C_6H_6^+$ isobar displays a significantly attenuated signal. Ion-specific images, displayed in Fig. 3, show that $C_2F_2O^+$ is uniformly distributed throughout the samples. As the dose of α particles increases, the signal of $C_2F_2O^+$ increases only within the irradiated portion of the samples. Conversely, ion-specific images of $(OH)_2SiO^+$ (see Fig. 3) show that this ion signal appears evenly distributed across the sample but with no appreciable change in signal within the irradiated portion of the sample as the α dose increases. These observations provide proof that, while $C_2F_2O^+$ is initially present as a fragment of perfluorinated polyether, the increase in signal is clearly the result of α particle irradiation. Furthermore, the dioxide species (e.g., $C_3F_3O_2^+$, $C_4F_3O_2^-$, and $C_3F_4O_2^-$) are found to be unique indicators of reaction between radiolytically generated fluorocarbon radicals and sources of oxygen.

Quantitative analysis of oxygen-functionalized fluorocarbon reaction products has been performed for both monoxide and dioxide species. The integrated signals of several dioxide species are plotted in Fig. 5. In this figure, the mean of the integrated signals of CFO_2^+ (63 m/z), $C_3F_3O_2^+$ (125 m/z), and $C_3F_4O_2^-$ (144 m/z) are plotted against the log of the dose. The mean values were calculated using data, excluding outliers, from all samples and are normalized to the total ion signals at each dose; the error bars indicate an interval of one standard deviation ($\pm 1\sigma$) from the mean. The data are fit from 10^7 to 5×10^{10} rad by the relationship $y=ae^{bx}$ where y is the normalized ion signal and x is $\log_{10}$ of the dose. The resulting slope and intercept of each curve, produced by fitting on a log-log scale, are CFO_2^+ (0.625, 0.25), $C_3F_3O_2^+$ (0.811, 1.35), and $C_3F_4O_2^-$ (0.794, 0.28). In general, the signals of dioxide fragments span several orders of magnitude over the experimental range of α doses, and the curves extrapolate very close to zero signal at zero dose. These data unambiguously show that dioxide species are not present in the virgin specimens, and arise only following irradiation of the sample with α particles.

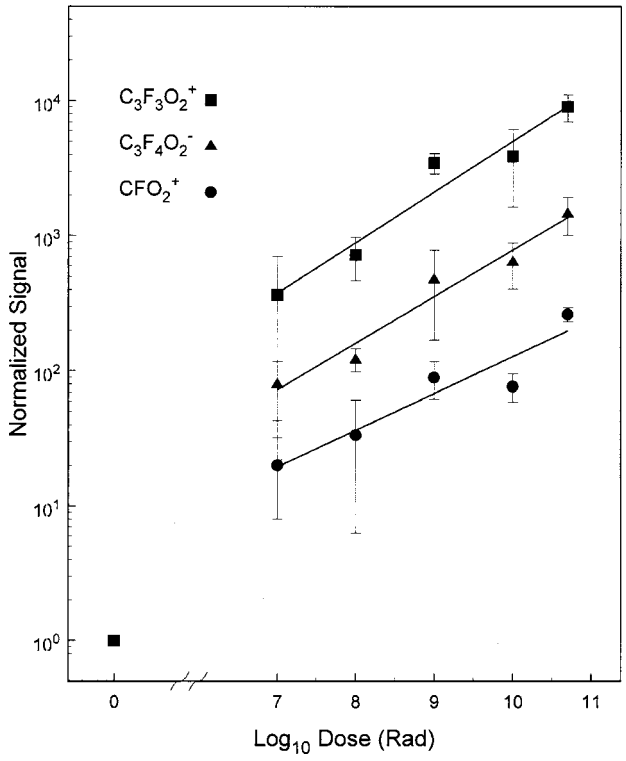

FIG. 5. Integrated counts of the peroxyl-functionalized fluorocarbon fragments CFO_2^+ (●), $C_3F_3O_2^+$ (■), and $C_3F_4O_2^-$ (▲) plotted as a function of α particle dose. The signals of these ions are zero at zero dose. The data are normalized to the total ion signal at each dose and are fit by the relationship $y=ae^{bx}$ over the experimental range of $10^7-5\times10^{10}$ rad. The resulting slopes and intercepts for each curve are given in the text. The residuals (R^2) are 0.84 for CFO_2^+, 0.95 for $C_3F_3O_2^+$, and 0.97 for $C_3F_4O_2^-$. The error bars indicate an interval of one standard deviation ($\pm 1\sigma$) from the mean.

The integrated signals of several monoxide species are plotted in Fig. 6. In this figure, the means of the integrated signals of $C_2F_2O^+$ (78 m/z), $C_3F_4O^+$ (128 m/z), and $C_3F_7O^+$ (185 m/z) are plotted as described for the dioxide species. The resulting slopes and intercepts of each curve, produced by fitting on a log-log scale, are $C_2F_2O^+$ (0.485, 129.89), $C_3F_4O^+$ (0.592, 76.25), and $C_3F_7O^+$ (0.375, 174.48). These data demonstrate that monoxide species are present in the unirradiated specimens, and that the signal of these species increases with increasing doses of α particles. However, the signals of the monoxide fragments only increase by one-half to one order of magnitude over the experimental range of α doses. Additionally, the slope of the curves of monoxide signals, approximately one-half that of the dioxide fragments, is an indication that the mechanism of formation may be distinct from that of the dioxide fragments.

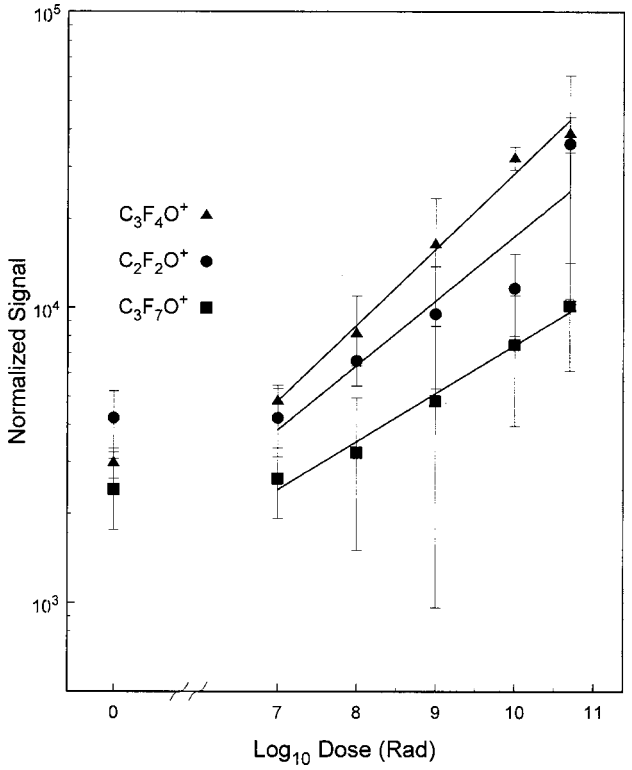

FIG. 6. Integrated counts of the oxyl-functionalized fluorocarbon fragments $C_2F_2O^+$ (●), $C_3F_4O^+$ (■), and $C_3F_7O^+$ (▲) plotted as a function of α particle dose. The data are normalized to the total ion signal at each dose and are fit by the relationship $y=ae^{bx}$ over the experimental range of $10^7-5\times10^{10}$ rad. The resulting slopes and intercepts for each curve are given in the text. The residuals (R^2) are 0.89 for $C_2F_2O^+$, 0.97 for $C_3F_4O^+$, and 0.99 for $C_3F_7O^+$. The error bars indicate an interval of one standard deviation ($\pm1\sigma$) from the mean.

IV. DISCUSSION

It has been demonstrated by Pasternak *et al.* that PTFE is permeable to small, noncondensable gas molecules by simple diffusion.[10] The observed diffusion was found to be independent of sample thickness and rather insensitive to temperature; however, the degree of crystallinity has been shown to have a demonstrable impact on the diffusion characteristics of linear polymers such as PTFE and polyethylene (PE).[11,12] Gases of H_2, N_2, O_2, and CO_2 were found to have permeability coefficients, P ($\times10^9$ cm^2/cm Hg s at STP), in PTFE of 0.98, 0.14, 0.42, and 1.17, respectively, while the heats of solution, ΔH_s, are negative and follow a similar trend. There are no available data regarding the permeability or heat of solution for CO or H_2O in PTFE, though a positive heat of solution has been established for CO in PE.[12]

Residual gas analysis indicates the presence of intercalated gas molecules that are liberated from PTFE during α particle irradiation. The samples were irradiated using a beam current of 40 nA which corresponds to a dose rate of 5×10^7 rad/s. The partial pressures of species at mass-to-charge ratios corresponding to H_2O^+ (18 m/z), CO^+/N_2^+ (28 m/z), O_2^+ (32 m/z), and CO_2^+ (44 m/z) were monitored concurrently during irradiation of the sample. The first indication of liberated gas molecules appeared at 5×10^{10} rad where a distinct increase in the partial pressures of H_2O^+, CO^+/N_2^+, and O_2^+ was observed. These gases, presumably sequestered within the polymer matrix and released when the matrix began to radiolytically decompose, provide a source of oxygen in PTFE with which radiolytically produced fluorocarbon radicals may react to form oxide moieties. Conspicuously absent from the RGA data was a rise in the partial pressure of CO_2. This result is contrary to expectation since PTFE has been shown to have a higher permeability to CO_2 than either N_2 or O_2.

The TOF-SIMS data bear evidence regarding the presence of H_2O, N_2, and O_2 in the PTFE matrix. The presence of H_2O is confirmed by signals at 18 m/z (H_2O^+) and 17 m/z (OH^+) in the positive polarity which are accompanied by a signal at 17 m/z (OH^-) in the negative polarity. The negative-ion spectra contain several peaks appearing at 19, 37, and 55 m/z identified as clusters having the structure $(H_2O)_nX^-$, where X is a solvated H^- or F^- ion that further supports the presence of water gas in the polymer matrix. The observation of CO_2^+ in the mass spectra is ascribed to perfluorinated polyether residues in the polymer matrix since CO_2H^+ is also observed. This supposition is supported by the RGA data which show an absence of a rise in the 44 m/z (CO_2^+) trace. The presence of molecular CO is questionable, at best, since a uniquely identifiable peak is not observed in the mass spectra at any level of α particle irradiation. Thus, the preponderance of evidence suggests that the vast majority of oxygen-containing gases present in the PTFE matrix consists of O_2, followed by H_2O. Molecular hydrogen is presumed to persist within the polymer matrix based on kinetic and thermodynamic data[10–12] as well as TOF-SIMS data.[1]

The dioxide species may be straightforwardly understood as products of reaction between α particle-generated fluorocarbon radicals and intercalated O_2 gas. For instance, a CF· radical may react with O_2 to yield CFO_2. This example provides an uncomplicated illustration of one possible pathway to a single product that is observed in the mass spectra. The monoxide species ostensibly arise from the three sources. First, monoxide species appear in the mass spectrum of unirradiated PTFE as indicators of perfluorinated polyether. Irradiation of the sample with α particles tends toward fragmentation of the perfluorinated polyether molecules, along with the PTFE matrix, which may contribute to the observed increase in the signal of monoxide fragments. However, the data generally indicate that the signals of decomposition products decay with increasing α dose.[1] Second, spontaneous (i.e., unimolecular) or induced (i.e., radiolytic) decomposition of dioxide moieties may contribute to the increase in the signals of monoxide species.[13] Third, the reaction of fluorocarbon radicals with atomic oxygen or O· radicals may contribute to the production of monoxide-functionalized fluorocarbons.[14]

The slopes of the monoxide curves are positive and, on average, one-half the magnitude of the dioxide curves indicating a second-order reaction mechanism. Therefore, a mechanism dominated by radiolytic decomposition of perfluorinated polyether molecules must be eliminated. Reactions

involving molecular oxygen, atomic oxygen, and O· radicals are second-order processes. Thus, we may conclude that the rise in monoxide signals with increasing α dose is the product of reaction between fluorocarbon radicals and molecular oxygen, atomic oxygen, or O· radicals, though at this time it is impossible to determine the degree to which each mechanism contributes to the observed signals. Reaction of radiolytically generated fluorocarbon radicals with molecular CO to form monoxide species is dismissed based on the rationale that has been articulated; namely, CO^+ is not discernable in the TOF-SIMS data.

V. CONCLUSIONS

We have elucidated the origin of monoxide- and dioxide-functionalized fluorocarbon species that emerge in the TOF-SIMS data upon irradiation of PTFE with MeV α particles. Monoxide fragments are observed in the mass spectra of unirradiated PTFE and are indicative of perfluorinated polyether residues. These residues presumably originate at some point during processing of the PTFE sheet stock used in these experiments. The rise in the signal of monoxide (oxyl) species with increasing α particle irradiation is most reasonably explained by reaction between fluorocarbon radicals and O_2, O, or O· radicals. The signals of dioxide (peroxyl) species arise in the mass spectra with the first dose of α particles and intensify with continued irradiation. The data suggest that dioxide species are solely the product of reaction between α particle-generated fluorocarbon radicals and molecular oxygen. We have identified N_2 gas in the PTFE matrix in addition to molecular water and oxygen; however, there are no species in the mass spectra that would indicate any sort of reaction between α particle-generated fluorocarbon radicals and molecular nitrogen. Perhaps degassing the experimental samples followed by exposure to, and α particle irradiation in, an N_2 atmosphere may affect resolution of this issue.

ACKNOWLEDGMENTS

One of the authors (G.L.F.) would like to acknowledge Chad Meserole for critical discussions and review of this manuscript. Financial support for this research was provided by the United States Department of Energy under Contract No. W-7405-ENG.

[1]G. L. Fisher, J. A. Ohlhausen, and C. J. Wetteland, Surf. Interface Anal. **37**, 713 (2005).
[2]G. L. Fisher, C. Szakal, C. J. Wetteland, and N. Winograd, J. Phys. Chem. (accepted).
[3]R. M. Braun, P. Blenkinsopp, S. J. Mullock, C. Corlett, K. F. Willey, J. C. Vickerman, and N. Winograd, Rapid Commun. Mass Spectrom. **12**, 1246 (1998).
[4]D. Weibel, S. Wong, N. Lockyer, P. Blenkinsopp, R. Hill, and J. C. Vickerman, Anal. Chem. **75**, 1754 (2003).
[5]D. Fischer, U. Lappan, I. Hopfe, K. J. Eichhorn, and K. Lunkwitz, Polymer **39**, 573 (1998).
[6]U. Lappan, U. Geißler, L. Haußler, D. Jehnichen, G. Pompe, and K. Lunkwitz, Nucl. Instrum. Methods Phys. Res. B **185**, 178 (2001).
[7]A. B. Ariawan, S. Ebnesajjad, and S. G. Hatzikiriakos, Powder Technol. **121**, 249 (2001).
[8]A. B. Ariawan, S. Ebnesajjad, and S. G. Hatzikiriakos, Polym. Eng. Sci. **42**, 1247 (2002).
[9]J. G. Newman, B. A. Carlson, R. S. Michael, and J. F. Moulder, *Static SIMS Handbook of Polymer Analysis* (Physical Electronics, Eden Prairie, 1991).
[10]R. A. Pasternak, M. V. Christensen, and J. Heller, Macromolecules **3**, 366 (1970).
[11]W. W. Brandt and G. A. Anysas, J. Appl. Polym. Sci. **7**, 1919 (1963).
[12]A. S. Michaels and H. J. Bixler, J. Polym. Sci. **50**, 393 (1961).
[13]U. Groß, P. Dietrich, G. Engler, D. Prescher, J. Schulze, K. Lunkwitz, and A. Ferse, J. Fluorine Chem. **20**, 33 (1982).
[14]Our data, to be disclosed in Ref. 2, indicate that α particles initiate reaction between H_2 and O_2 to form H_2O_2 which decomposes to H_2O and O.